THE JOURNAL OF PHYSICAL CHEMISTRY B LETTERS

2007, *111,* 6992−6997
Published on Web 05/31/2007

Crystallization Behavior of Soft, Attractive Microgels

Zhiyong Meng,[†] Jae Kyu Cho,[‡] Stella Debord,[†] Victor Breedveld,[‡] and L. Andrew Lyon*,[†]

School of Chemistry and Biochemistry and Petit Institute for Bioengineering and Bioscience, Georgia Institute of Technology, Atlanta, Georgia 30332-0400, School of Chemical and Biomolecular Engineering, Georgia Institute of Technology, Atlanta, Georgia 30332-0100

Received: April 23, 2007; In Final Form: May 15, 2007

The equilibrium phase behavior and the dynamics of colloidal assemblies composed of soft, spherical, colloidal particles with attractive pair potentials have been studied by digital video microscopy. The particles were synthesized by precipitation copolymerization of *N*-isopropylacrylamide (NIPAm), acrylic acid (AAc), and *N*,*N*′-methylene bis(acrylamide) (BIS), yielding highly water swollen hydrogel microparticles (microgels) with temperature- and pH-tunable swelling properties. It is observed that in a pH = 3.0 buffer with an ionic strength of 10 mM, assemblies of pNIPAm−AAc microgels crystallize due to a delicate balance between weak attractive and soft repulsive forces. The attractive interactions are further confirmed by measurements of the crystal melting temperatures. As the temperature of colloidal crystals is increased, the crystalline phase does not melt until the temperature is far above the lower critical solution temperature (LCST) of the microgels, in stark contrast to what is typically observed for phases formed due to purely repulsive interactions. The unusual thermal stability of pNIPAm−AAc colloidal crystals demonstrates an enthalpic origin of crystallization for these microgels.

Colloidal particles are receiving growing attention in the scientific and industrial communities due to their value as model systems in condensed matter physics[1] and their industrial applicability[2] in paints,[3] sensors,[4] and drug delivery.[5] Colloidal particles can be thought of as "big atoms"[6] in a continuous medium that mimic the interactions, thermodynamics, and dynamics of atoms or molecules in gas, liquid, and solid phases. Quantitative methodologies to approach the pair interactions of charge stabilized colloidal particles were originally developed by Derjaguin and Landau[7] and Verwey and Overbeek[8] (DLVO theory). Furthermore, Kirkwood[9] and McMillan[10] developed a coarse-graining framework in which the correlation of equilibrium properties of colloidal dispersions with effective pair potentials is used to calculate the phase behavior and structure of colloidal assemblies. In these theoretical treatments, colloidal particles are categorized by the shape of their interparticle pair potential curve, wherein the interactions can be classified as hard spheres,[1] sticky hard spheres,[11] and soft spheres.[12] On the other hand, chemists have developed methods for the synthesis of particles that can act as experimental models to verify theoretical predictions[13] and computer simulations.[14] Sterically stabilized poly(methyl methacrylate) (PMMA)[14] and silica particles[15] have been used as model systems for hard spheres and sticky hard spheres to illustrate the phase behavior of colloidal assemblies with different pair interactions between particles. Recently, poly(*N*-isopropylacrylamide) (pNIPAm)-based microgels[16] have emerged as potentially useful model soft spheres due to the tunability of their softness and volume as a function of temperature. Soft repulsive interactions arising from repulsion[17] between coronas around pNIPAm particles and the deformability[18] of pNIPAm particles confer to pNIPAm colloidal dispersions the ability to exhibit richer phase behavior than hard sphere colloids.[19] The temperature-induced volume phase transition of pNIPAm provides a relatively simple experimental variable with which the effective volume fraction occupied by the microgels in a dispersion can be modulated.[20] Furthermore, the incorporation of acrylic acid (AAc) moieties into pNIPAm particles adds pH- and ionic strength-tunability,[16,21−27] giving rise to even more complex phase behavior. Ionic strength, pH, temperature, and medium composition have been found to affect the pair interactions of these colloidal particles.[16,21]

In this contribution, we report the colloidal crystallization behavior of pNIPAm−AAc microgels cross-linked with *N*,*N*′-methylene bis(acrylamide) (BIS). The synthesis, purification, and self-assembly of BIS-cross-linked pNIPAm−AAc microgel particles have been reported previously by our group.[25−27] For the specific studies reported here, the particles were composed of 84 mol % NIPAm, 15 mol % AAc, and 1 mol % BIS, and their typical size is about 1.5 μm in a pH 3.00 buffer, as determined by Cumulants analysis of dynamic light scattering (DLS, Protein Solutions) data. For these particles, the polydispersity was <10% by DLS. Dispersions were studied in a formate buffer at pH 3.00 with an ionic strength of 10 mM over temperatures ranging from 20 to 45 °C. All studies performed at a fixed temperature were done at 20 °C unless otherwise noted. The ionic strength is controlled by adding an appropriate amount of NaCl. At this pH, which lies below the pK_a (4.25) of AAc moieties, Coulombic repulsion between ionized microgels is minimized. As a result, the interparticle

* To whom correspondence should be addressed: LL62@mail.gatech.edu.
[†] School of Chemistry and Biochemistry and Petit Institute for Bioengineering and Bioscience.
[‡] School of Chemical and Biomolecular Engineering.

10.1021/jp073122n CCC: $37.00

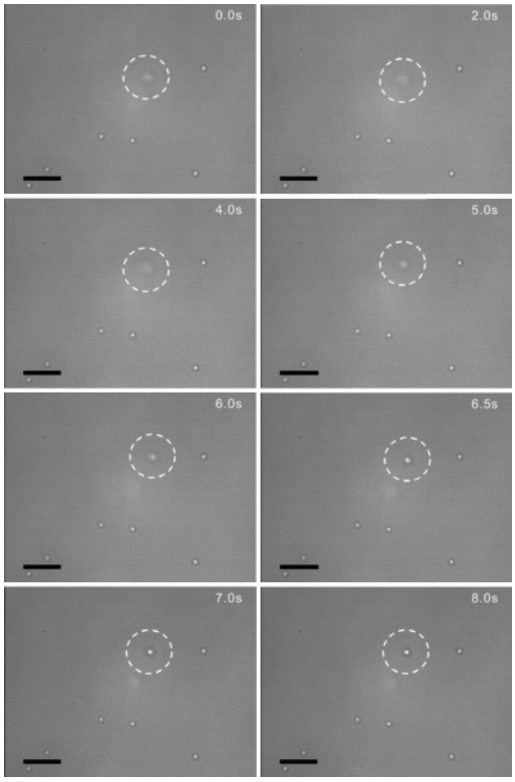

Figure 1. Microscopy images of the adhesion of pNIPAm−AAc microgel particles (0.01 wt % dispersion) to a glass surface (inner surface of a capillary) in a pH = 3.00, I = 10 mM aqueous buffer. The in situ recording of the attachment is strong evidence of the stickiness of pNIPAm−AAc microgel particles. Note the presence of multiple particles that have already adhered to the glass. The scale bar = 10 μm.

potential should be dominated by soft repulsion due to excluded volume interactions and steric hindrance, balanced by attraction due to hydrogen bonding[28,29] and van der Waals forces.[30] Note that due to weak attractive interactions between these microgels and difficulties in the evaluation of the "true" volume fractions of pNIPAm−AAc microgels with diffuse coronal regions,[17] the use of (effective) volume fraction as a parameter to describe the phase behavior of pNIPAm−AAc microgels would be speculative. Instead, in this contribution, we use the weight concentration of microgels to illustrate the phase behavior.[31]

The research presented here was motivated by an initial observation made during tracking experiments of dilute suspensions, in which we noticed the propensity of pNIPAm−AAc microgels to adhere to hydrophilic interfaces. An Olympus IX-71 microscope and Andor LUCA^{EM} camera equipped with an electron multiplying charge-coupled device (EMCCD) were used to monitor and record the motion of microgels. Figure 1 shows a series of images obtained from a dilute (<0.10 wt %) dispersion of pNIPAm−AAc microgels at 20 °C. The figure shows the irreversible adsorption of particles with an average diameter of ∼1.5 μm on the inner surface of the rectangular glass capillary (0.1 mm × 2.0 mm × 50 mm, Vitrocom). The observation of microgel adhesion was consistent throughout our experiments; when diffusing microgels came into close proximity to the glass surface, they were always found to irreversibly adsorb. Indeed, in Figure 1, all of the other microgels in the field of view are adsorbed to the glass surface. Over long times, all microgel particles from such dilute dispersions stick to the inner walls of the capillary and the solution becomes depleted of particles. The adhesion of pNIPAm−AAc microgels to the glass surface of the capillary suggests a net attractive interaction between the particles and glass surface. The hydroxyl groups on the glass surface have a negligible charge density at this pH, and the net attraction cannot be attributed to electrostatic interactions. Instead, the primary driving force is most likely hydrogen bonding between hydroxyl groups and carboxylic acid or amide groups on the particles, as well as van der Waals interactions.

In addition, in these dilute solutions, we also find attractive *interparticle* potentials, indicated by the formation of small aggregates (∼2−6 particles) *without* extensive flocculation; this is in agreement with previous reports on the coagulation of pNIPAm-based microgels.[32] Although one would expect a strong electrostatic repulsion between particles at high pH, at pH 3.00, where only ∼5% of the AAc carboxylic acid groups are predicted to be deprotonated, the interactions between the particles are believed to be affected by hydrogen bonding between NIPAm moieties and/or AAc moieties on the pNIPAm−AAc microgels.[28]

When the concentration of microgels is increased further, the behavior of the dispersion changes from that of a colloidal gas to a colloidal liquid. To enable quantification of particle motion, the microgel positions in an image time series acquired *via* video microscopy were analyzed using a modified version of the particle tracking code originally developed by Crocker and Grier[33] in the IDL (Research System, Inc.) programming environment. From statistical analysis of the particle motion, the mean-squared displacement (MSD) can be calculated as a function of lag time. This method of data analysis allows for quantitative evaluation of the dynamics and phase behavior of colloidal dispersions. The MSD of particles in an ensemble is given by

$$\mathrm{MSD}(\tau) = \langle (r_i(t+\tau) - r_i(t))^2 \rangle_{i,t} \quad (1)$$

where $r_i(t)$ is the position vector of the ith particle at time t, τ is the lag time, and $\langle\rangle_{i,t}$ indicates the average over the ensemble of particles as well as all starting times t. In the liquid regime, where the particle motion is expected to be purely diffusive, the MSD should be proportional to lag time:

$$\mathrm{MSD}(\tau) = 2dD\tau \quad (2)$$

where d is the dimensionality of the displacement vectors and D is the self-diffusion coefficient. The movies of the three-dimensional (3D) colloidal crystals studied here only provide access to a projection of particle trajectories in two dimensions and therefore $d = 2$ for video microscopy of a single crystal plane.[33] In general, the MSD is expected to scale with lag time according to

$$\mathrm{MSD}(\tau) \propto \tau^{\beta} \quad (3)$$

where the scaling parameter β is the slope in a double-logarithmic plot of MSD versus τ. In general, $\beta = 1$ for purely diffusive motion, β values between 0 and 1 denote subdiffusive behavior, and $\beta = 2$ for ballistic motion.

Figure 2a and b shows the MSD (a) and the local slope β (b) as a function of lag time for pNIPAm−AAc dispersions ranging in concentration from 2.0 to 8.0 wt %. Figure 3 shows the corresponding microscopic images and particle trajectories (determined over 60 s). With an increased weight fraction of pNIPAm−AAc microgels in the dispersion (from top to bottom in Figure 3), the dispersion displays the following phases: diffusive liquid → subdiffusive liquid → crystal → glass, which agrees with previous theoretical predictions[34] and other experiments.[35] Visual inspection of the MSD data (Figure 2a) and

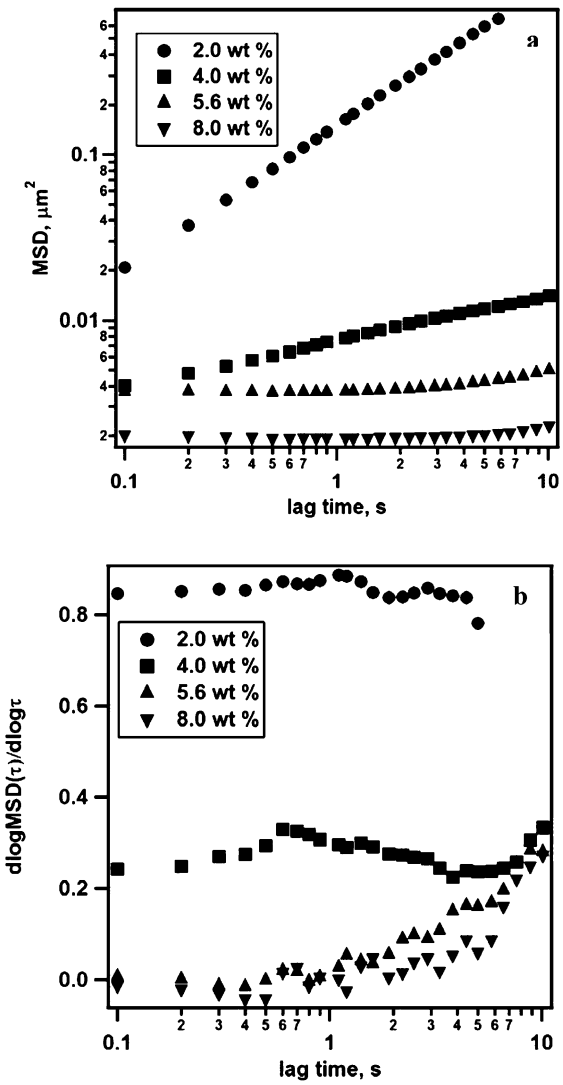

Figure 2. MSD profiles of pNIPAm−AAc microgel dispersions with different weight percentages in aqueous buffer at pH = 3.00 and I = 10 mM. (a) Log−log time evolution of quasi-2D mean square displacement (MSD). (b) Time evolution of the derivative of the log−log time evolution of quasi-2D MSD versus lag time.

trajectories (Figure 3) suggests that diffusive behavior is observed for pNIPAm−AAc dispersions at 2.0 wt %. However, determination of β yields values of ∼0.85 (see Figure 2b) for this sample. This indicates slightly subdiffusive behavior in the colloidal dispersion; this is most likely a result of hydrodynamically coupled interparticle interactions between the microgels.[36]

One of the key parameters that can be derived from Figure 2b is the structural relaxation time τ_R, a measure for the time it takes particles to move over a distance equal to their own radius. Extrapolation of Figure 2a yields a structural relaxation time τ_R of ca. 60 s for the 2.0 wt % sample, a time scale that is easily observed by video microscopy. Upon increasing the microgel concentration to 4.0 wt %, the microgels show strongly subdiffusive behavior with $\beta \sim 0.25$. At these concentrations, the dispersions show a caging effect due to the close proximity of the neighboring particles. The motion is thus much slower than the Brownian diffusion in the 2.0 wt % sample. At a concentration of 5.6 wt %, the dispersion displays crystalline iridescence, and the ordered (111) face of a face cubic centered lattice is observed in the microscopy image (Figure 3). Under these conditions, the MSD reaches a plateau at long lag times due to the caging effect imposed by neighboring particles in

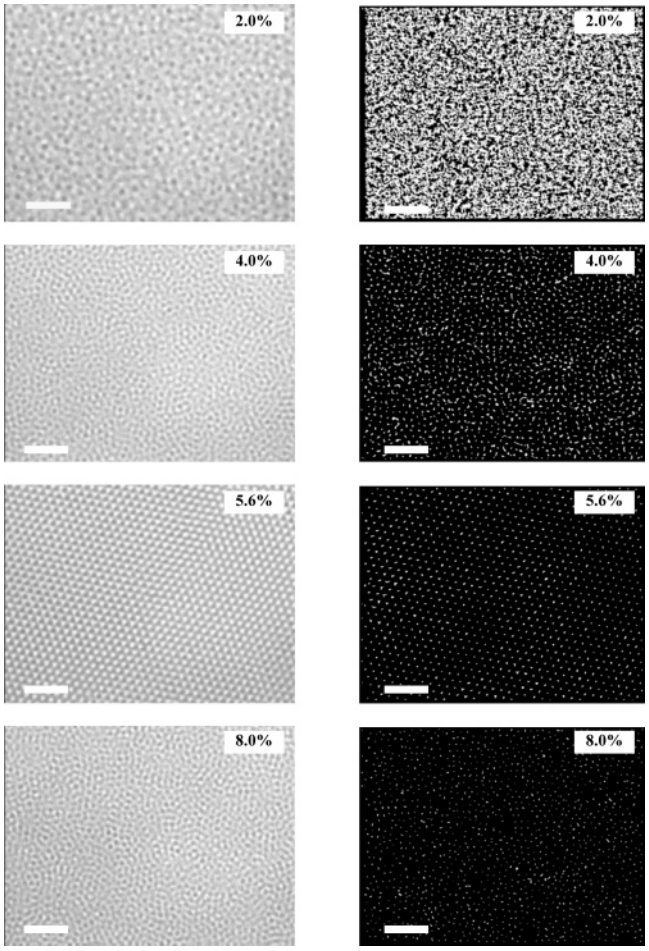

Figure 3. Microscopy images (left) and trajectories (right) of microgel dispersions at different concentrations from 2.0 up to 8.0 wt %. The scale bar = 10 μm. For all trajectory maps, the experimental time scale is 60 s.

the lattice. Thus, the values of β are effectively 0 for this sample and the particle motion consists only of thermal vibration around the lattice sites. At 8.0 wt % pNIPAm−AAc, the microgels appear to be jammed into a nearly motionless, unordered colloidal glass at short times. For both the crystalline (5.6 wt %) and glassy sample (8.0 wt %), the relaxation time τ_R diverges at longer times.

The data presented above is suggestive of both particle−surface attractions (Figure 1) and weak interparticle attractions (subdiffusive liquid phase and a narrow crystallization regime). Even more compelling evidence of attractive interactions between the microgels comes from measurements of the crystal melting points. As reported by Hu[20] and his collaborators, pNIPAm microgel crystals typically melt at ∼26 °C (slightly below the lower critical solution temperature, LCST, of pNIPAm, ∼31 °C) due to microgel deswelling. Small amounts of thermally induced deswelling reduce the effective volume fraction of the assembly, thereby driving a transition from the crystal phase to the fluid region of the phase diagram. Specifically, when the effective microgel volume fraction goes below 0.495 during deswelling, the microgel crystalline phase melts and a fluid phase emerges. However, the melting points of the pNIPAm−AAc microgel crystals we have studied are much higher than the intrinsic LCST of the particles (∼32 °C). The heating profile for a 5.6 wt % pNIPAm−AAc microgel phase is shown in Figure 4. These data show that, even at 43 °C, where microgel particles in dilute suspensions have a 56% smaller hydrodynamic radius than that at 20 °C, the crystalline phase

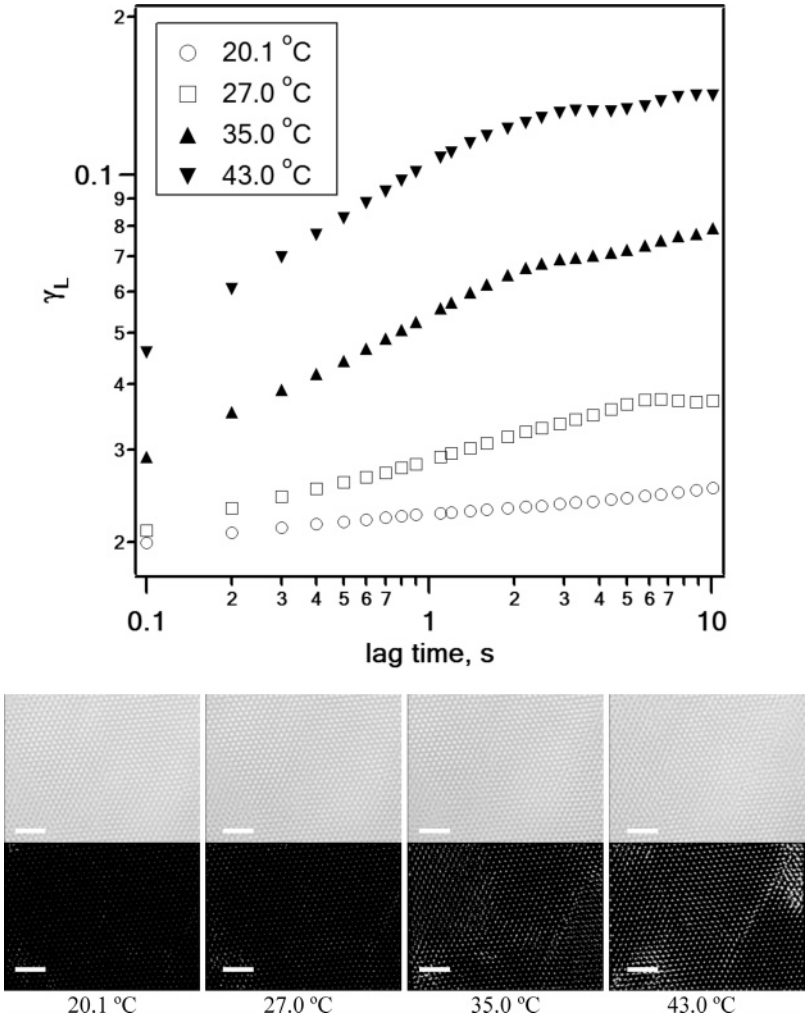

Figure 4. Temperature profile of the Lindemann parameter of pNIPAm−AAc colloidal crystals (5.6 wt %) versus lag time (pH = 3.00, I = 10 mM). The images are the microscopy images (top) and trajectories (bottom) of microgel dispersions at different temperatures from 20.1 to 43.0 °C. The scale bar = 10 μm.

becomes only slightly more mobile. If microgel deswelling in the concentrated dispersion was the same as in the dilute dispersion, the effective dispersion volume fraction should have decreased by 91%. In that scenario, the 5.6 wt % sample at 43 °C should be equivalent to a 0.5 wt % sample at 20 °C, which would be a fluid according to Figure 2. The presence of crystalline structure far above the microgel LCST suggests the presence of a strong attractive interaction potential between the particles that stabilize the assembly against melting, in contrast to pure pNIPAm crystals which readily melt upon deswelling.[20]

To quantitatively assess the crystal melting, we invoke the Lindemann criterion. The 2D Lindemann parameter is defined as

$$\gamma_L(\tau) = \frac{\sqrt{\mathrm{MSD}(\tau)}}{a} \quad (4)$$

where a is the center-to-center distance between particles. The 2D Lindemann parameter is a measurement of positional fluctuations of colloidal particles relative to the crystal lattice spacing and is a function of the concentration of particles as well as environmental factors such as temperature. In samples where particles are caged by their nearest neighbors, the MSD-(τ) asymptotically approaches a constant value, and the corresponding Lindemann parameter is lower than the critical Lindemann parameter. When the particles are able to rearrange, the MSD(τ) increases with time, and the corresponding Lindemann parameter becomes higher than the critical Lindemann parameter, γ_L^c; for an FCC (face-centered cubic) crystal with a DLVO-form potential γ_L^c = 0.16−17.[37,38] Note that while a pure FCC phase is assumed based on our previous work on similar crystals, even if the crystal contains some HCP (hexagonal close packing) structure, the critical Lindemann parameter for melting will not be significantly affected.[39,40]

The evolution of the Lindemann parameter for the 5.6 wt % dispersion of pNIPAm−AAc microgels as a function of temperature and lag time is presented in Figure 4; the values increase with both temperature and lag time. From DLS, the diameter of pNIPAm−AAc colloidal particles in a pH 3.00 buffer is ∼1.5 μm at 20 °C, and the spacing between the nearest particles in colloidal crystals is about 1.8 μm according to radial distribution function, $g(r)$, at 20 °C (data not shown). We find that even at 43 °C, the corresponding Lindemann parameter is 0.161, which barely exceeds the critical Lindemann parameter for melting. This is in agreement with the stable crystal structure observed from the corresponding microscopy image and trajectories. We also conducted a thermal stability analysis for the subdiffusive pNIPAm−AAc dispersion at 4.0 wt %. As shown in Figure 5, the microgels show subdiffusive behavior with a Lindemann parameter of 0.158 at 34 °C. Due to the lack of a critical Lindemann parameter for the subdiffusive-to-diffusive fluid transition, it is impossible to rigorously define a "melting

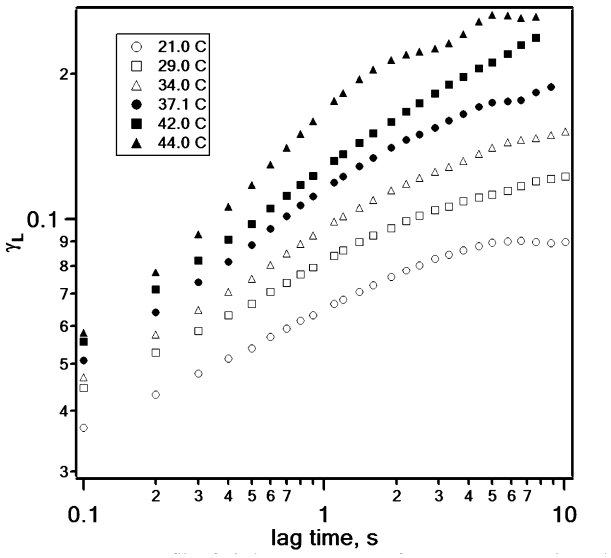

Figure 5. Temperature profile of the Lindemann parameter for pNIPAm−AAc microgel subdiffusive fluids with a concentration of 4.0 wt % in an aqueous buffer (pH = 3.00, I = 10 mM). Open symbols correspond to subdiffusive behavior, whereas filled symbols correspond to diffusive behavior.

point" for the transition between a dense subdiffusive colloidal liquid and a diffusive liquid. Thus, to a first approximation, we use the critical Lindemann parameter for a crystal−liquid transition to determine subdiffusive-to-diffusive fluid transition. Because the Lindemann parameter for 4.0 wt % pNIPAm−AAc microgels at 34 °C is below 0.16, our results suggest that the microgels are still subdiffusive, indicating that there is also some thermal stability to this phase. As with the crystal phase, this is presumably due to interparticle attractions between pNIPAm−AAc microgels.

From the phase behavior shown above for concentrated dispersions, we conclude that the crystallization of pNIPAm−AAc microgels at pH 3.0 occurs in a narrow concentration range (5.6−6.5 wt %) between a dense, subdiffusive liquid and a jammed glass. The mechanistic understanding of soft colloidal crystallization is ongoing in our group; for the materials in this study, crystallization is the result of a delicate balance between repulsive and attractive interactions. The soft repulsive interaction presumably has three sources; one is the solvation repulsion between solvated pNIPAm−AAc coronas around the particles, another is the compression and/or interpenetration of pNIPAm−AAc coronas, and the last is the deformation of microgels upon close contact. In addition to soft repulsive interactions, electrostatic repulsion between deprotonated carboxylate groups and residual sulfate groups (from the persulfate initiator used) also contributes to the total repulsion between pNIPAm−AAc particles. On the other hand, attractive interactions can be attributed to three forces: van der Waals attractions, hydrogen bonding between protonated carboxylic acid groups and/or amide groups and the surfaces of neighboring microgels, and hydrophobic interactions between isopropyl groups and/or the main chain of pNIPAm−AAc coronas. Given the temperature dependencies of both hydrogen bonding and hydrophobic interactions, we expect that if both are contributing significantly to the observed phase behavior, the hydrogen-bonding would be more important at temperatures below the pNIPAm LCST, while hydrophobic interactions may become important above the LCST.

Given this situation, it is likely that when the suspension of pNIPAm−AAc microgels becomes more concentrated, the total interaction[30] between two microgels becomes dominated by short-range interactions such as hydrogen bonding[28] and/or hydrophobic interaction.[41] However, due to the existence of the soft repulsive interactions and electrostatic repulsion, the initial potential well due to the attractive interaction is apparently not very deep and may be very close to thermal energy k_BT, as evidenced by the lack of extensive microgel aggregation in these dispersions. Also, an additional potential barrier due to steric and Coulombic repulsive interactions would reduce the probability of aggregation of particles in the suspension appreciably. However, if two particles approach to close contact, the potential well arising from short-range hydrogen bonding interactions will hold the two particles together, while thermal fluctuations will tend to dissociate the aggregates. It is likely, therefore, that these weak interparticle attractions permit crystallization, as opposed to frustrating it, due to a delicate balance between the potential energy well-depth and the bath temperature. Dynamic association and dissociation of particle assemblies will allow for an overall minimization of the Gibbs free energy, thereby driving the assembly to a crystalline arrangement over that narrow range of packing densities (5.6−6.5 wt %). As one would expect from this model, a disordered glassy phase is formed at higher concentrations, where the diffusion of the attractive spheres is frustrated due to the high viscosity of the dispersion and the global minimum cannot be accessed.

Furthermore, the thermostability of pNIPAm−AAc colloidal crystals can be rationalized by the attractive interactions, presumably due to hydrogen bonding between the AAc moieties and/or NIPAm moieties and hydrophobic interactions[41] among isopropyl groups. At a specific center-to-center distance, the potential well that stabilizes the configuration of colloidal particles in the condensed phase becomes deeper due to the favorable rearrangement of AAc and/or NIPAm moieties on the dangling chains at the surface of pNIPAm−AAc colloidal particles. For an FCC or HCP structure, the particle in an interior lattice cell will have 12 nearest neighbors, which presumably create a potential well with a depth of about $12k_BT$. In this fashion, we can rationalize the thermal stability of pNIPAm−AAc colloidal crystals. Thus, the melting temperature is much higher than that of the pNIPAm crystalline phase due to the excess enthalpic contribution to the Gibbs free energy for the solid−liquid phase transition. The above argument is also valid for the unexpected thermostability of the subdiffusive dense fluid, in which interparticle distances are small, as well.

In summary, the analysis of the dynamics of concentrated pNIPAm−AAc colloidal dispersions demonstrates short-range attractions between particles, which contribute to the crystallization of pNIPAm−AAc microgels at pH 3.00 and the thermal stability of the resulting colloidal crystals. The delicate balance between soft repulsion and short-range weak attraction due to hydrogen bonding and/or van der Waals interactions drive the pNIPAm−AAc colloids to form polycrystalline phases. The thermal stability of the dense colloidal fluids and crystals is attributed to the additivity of an attractive potential well due to hydrogen bonding (<LCST) and/or hydrophobic interactions (>LCST) and the rearrangement of pNIPAm−AAc coronas upon close contact, thereby lowering the local Gibbs free energy. Given the above phenomena, we expect that pNIPAm−AAc microgel particles will serve as an excellent model for pH- and temperature-tunable colloids in future studies on the complex phase behavior and dynamics of colloidal dispersions.

Acknowledgment. L.A.L. acknowledges financial support from the Dreyfus Foundation, the Office of Naval Research, and the ONR DURIP program for this work (N00014-03-1-

0225 and N00014-04-1-0488); V.B. acknowledges support from the National Science Foundation (CAREER award, CTS-0547066).

References and Notes

(1) Hoover, W. G.; Ree, F. H. *J. Chem. Phys.* **1968**, *49*, 3609.
(2) Tadros, T. F. *Adv. Colloid Interface Sci.* **1998**, *46*, 1.
(3) Castelvetro, V.; De Vita, C. *Adv. Colloid Interface Sci.* **2004**, *108*−*109*, 167.
(4) De Rossi, D.; Carpi, F.; Scilingo, E. P. *Adv. Colloid Interface Sci.* **2005**, *116*, 165.
(5) Kogan, A.; Garti, N. *Adv. Colloid Interface Sci.* **2006**, *123*−*126*, 369.
(6) Poon, W. *Science* **2004**, *304*, 830.
(7) Derjaguin, B. V.; Landau, L. D. *Acta Physicochimica URSS* **1941**, *14*, 633.
(8) Verwey, E. J. W.; Overbeek, H. N. W. *Theory of the stability of lyophobic colloids*; Elsevier: Amsterdam, 1948.
(9) Kirkwood, J. G.; Buff, F. P. *J. Chem. Phys.* **1951**, *19*, 774.
(10) McMillan, W. G. J.; Mayer, J. E. *J. Chem. Phys.* **1945**, *13*, 276.
(11) Baxter, R. J. *J. Chem. Phys.* **1968**, *49*, 2770.
(12) Cape, J. N.; Finney, J. L.; Woodcock, L. V. *J. Chem. Phys.* **1981**, *75*, 2366.
(13) Pusey, P. N. Colloidal suspensions. In *Liquids, Freezing and Glass Transition*; Hansen, J. P., Levesque, D., Zinn-Justin, J., Eds.; North-Holland: Amsterdam, 1989; Vol. 51, pp 763.
(14) Pusey, P. N.; van Megen, W. *Nature* **1986**, *320*, 340.
(15) Jansen, J. W.; de Kruif, C. G.; Vrij, A. *J. Colloid Interface Sci.* **1986**, *114*, 471.
(16) Snowden, M. J.; Chowdhry, B. Z.; Vincent, B.; Morris, G. E. *J. Chem. Soc., Faraday Trans.* **1996**, *92*, 5013.
(17) Bartsch, E.; Kirsch, S.; Lindner, P.; Scherer, T.; Stölken, S. *Ber. Bunsen*−*Ges. Phys. Chem.* **1998**, *102*, 1597.
(18) Bartsch, E.; Frenz, V.; Baschnagel, J.; Schärtl, W.; Sillescu, H. *J. Chem. Phys.* **1997**, *106*, 3743.
(19) Debord, S. B. Phase behavior of multiresponsive microgel dispersions. Ph.D. Dissertation, Georgia Institute of Technology, Atlanta, 2005.
(20) Wu, J.; Zhou, B.; Hu, Z. *Phys. Rev. Lett.* **2003**, *90*, 048304.
(21) Kratz, K.; Hellweg, T.; Eimer, W. *Ber. Bunsen*−*Ges. Phys. Chem.* **1998**, *102*, 1603.
(22) Kokufuta, E.; Wang, B.; Yoshida, R.; Khokhlov, A. R.; Hirata, M. *Macromolecules* **1998**, *31*, 6878.
(23) Suzuki, H.; Wang, B.; Yoshida, R.; Kokufuta, E. *Langmuir* **1999**, *15*, 4283.
(24) Fernández-Nieves, A.; Fernández-Barbero, A.; Vincent, B.; de las Nieves, F. J. *Macromolecules* **2000**, *33*, 2114.
(25) Jones, C. D.; Lyon, L. A. *Macromolecules* **2000**, *33*, 8301.
(26) Debord, S. B.; Lyon, L. A. *J. Phys. Chem. B* **2003**, *107*, 2927.
(27) Lyon, L. A.; Debord, J. D.; Debord, S. B.; Jones, C. D.; McGrath, J. G.; Serpe, M. J. *J. Phys. Chem. B* **2004**, *108*, 19099.
(28) Scheiner, S. *Hydrogen Bonding: A Thereotical Perspective*; Oxford University Press: New York, 1997.
(29) Pham, K. N.; Puertas, A. M.; Bergenholtz, J.; Egelhaaf, S. U.; Moussaid, A.; Pusey, P. N.; Cates, M. E.; Fuchs, M.; Poon, W. C. K. *Science* **2002**, *296*, 104.
(30) Hunter, R. J. *Foundations of Colloid Science*, 2nd ed.; Oxford University Press: Oxford, Great Britain, 2001.
(31) Wu, J.; Zhou, B.; Hu, Z. *Phys. Rev. Lett.* **2003**, *90*, 048304.
(32) Makino, K.; Kado, H.; Ohshima, H. *Colloids Surf. B: Biointerfaces* **2001**, *20*, 347.
(33) Crocker, J. C.; Grier, D. G. *J. Colloid Interface Sci.* **1996**, *179*, 298.
(34) Bengtzelius, U.; Götze, W.; Sjölander, A. *J. Phys. C: Solid State Phys.* **1984**, *17*, 5915.
(35) Pham, K. N.; M., P. A.; Bergenholtz, J.; Egelhaaf, S. U.; Moussaïd, A.; Pusey, P. N.; Schofield, A. B.; Cates, M. E.; Fuchs, M.; Poon, W. C. K. *Science* **2002**, *296*, 104.
(36) Jones, R. B.; Pusey, P. N. *Annu. Rev. Phys. Chem.* **1991**, *42*, 137.
(37) Saija, F.; Prestipino, S.; Giaquinta, P. V. *J. Chem. Phys.* **2006**, *124*, 244504.
(38) Kuhn, P. S.; Diehl, A.; Levin, Y.; Barbosa, M. C. *Physica A* **1999**, *247*, 235.
(39) Cho, S.-A. *J. Phys. F: Met. Phys.* **1982**, *12*, 1069.
(40) Alsayed, A. M.; Islam, M. F.; Zhang, J.; Collings, P. J.; Yodh, A. G. *Science* **2005**, *309*, 1207.
(41) Ishida, N.; Kobayashi, M. *J. Colloid Interface Sci.* **2006**, *297*, 513.